

informed consent from IV drug abusers in New Orleans who were attending the Desire Narcotics Rehabilitation Center), and peripheral blood mononuclear cells were isolated by Ficoll-Hypaque density gradient centrifugation (at UCLA and Abbott Laboratories). The peripheral blood mononuclear cells were cryopreserved until further analysis. Preparation of all blood samples and storage were performed with the use of facilities and reagents specifically designated for PCR analysis. DNA was prepared from approximately  $10^7$  cryopreserved cells by SDS-proteinase K treatment, followed by phenol and chloroform extraction. DNA was analyzed by PCR (10) with the following modification. Samples were subjected to PCR analysis for 30 cycles (40 cycles for DNA sequence analysis) with 100 ng of each primer, including  $5 \times 10^6$  cpm of one primer labeled at the 5' end with [ $\gamma$ - $^{32}$ P]ATP. Reactions were performed in 25 mM tris-HCl, pH 8.0, 5 mM MgCl<sub>2</sub>, 50 mM NaCl, and 0.25 mM each of deoxyadenosine triphosphate, deoxycytidine triphosphate, deoxythymidine triphosphate, and deoxyguanosine triphosphate in a total volume of 25  $\mu$ l, cycling at 65°C for 2 min and at 91°C for 1 min. After amplification, 5  $\mu$ l of the reaction were used for further analysis by 8% polyacrylamide gel electrophoresis. With these modifications, the PCR prod-

ucts could be visualized directly after gel electrophoresis and autoradiography, without a need for additional hybridization steps. Exposure times varied from 2 to 12 hours, depending on the intensity of the signal. Oligonucleotide primers corresponding to the *tax/rex* region of HTLV-I were used to detect both HTLV-I and HTLV-II sequences. Oligonucleotides from the *pol* gene region that specifically detect either HTLV-I or HTLV-II were also tested in some cases. The possibility of false positives because of the extreme sensitivity of the PCR method was excluded for the following reasons: (i) DNA preparation and PCR reactions were performed in a separate facility from the location where the PCR products were analyzed. (ii) All reagents were specifically designated for PCR analysis and used exclusively for that purpose. (iii) Negative control samples were included in parallel at each step, from purification of blood mononuclear cells through PCR analysis. (iv) Results from some samples were confirmed with a second lymphocyte isolation and prepared in geographically distinct laboratories.

14. A. M. Maxam and W. Gilbert, *Proc. Natl. Acad. Sci. U.S.A.* **74**, 560 (1977).
15. D. B. Duggan *et al.*, *Blood* **71**, 1022 (1988); S. Bhagavati *et al.*, *N. Engl. J. Med.* **318**, 1141 (1988).
16. K. T. A. Malik, J. Eveir, A. Karpas, *J. Gen. Virol.*

**69**, 1695 (1988); L. Ratner, *J. Virol.* **54**, 781 (1985); H. Tsujimoto, *Mol. Biol. Med.* **5**, 29 (1988); HTLV-II<sub>Mo</sub> and HTLV-II<sub>NRA</sub> show 99% homology in the long terminal repeat (I. S. Y. Chen and J. D. Rosenblatt, unpublished data).

17. I. S. Y. Chen *et al.*, *Proc. Natl. Acad. Sci. U.S.A.* **80**, 7006 (1983); T. N. Chosa *et al.*, *Gann* **73**, 844 (1982); I. Miyoshi *et al.*, *ibid.* **72**, 997 (1981); M. Popovic *et al.*, *Proc. Natl. Acad. Sci. U.S.A.* **80**, 5402 (1983); N. Yamamoto *et al.*, *Science* **217**, 737 (1982).
18. J. M. Jason, J. S. McDougal, C. Cabradilla, V. S. Kalyanaraman, B. L. Evatt, *Am. J. Hematol.* **20**, 129 (1985); G. Y. Minamoto *et al.*, *N. Engl. J. Med.* **318**, 219 (1988); K. Miyamoto *et al.*, *Int. J. Cancer* **33**, 721 (1984); K. Okochi, H. Sato, Y. Hinuma, *Vox Sang.* **46**, 245 (1984).
19. We thank E. Chin, J. Q. Zhao, A. Diagne, S. Weitsman, and J. Breister for technical assistance; W. Aft and J. Stark for preparation of the manuscript; and J.-P. Allain for helpful comments on the manuscript. Supported in part by grants from the National Cancer Institute, the American Cancer Society, and the University of California-wide AIDS task force.

22 December 1988; accepted 27 February 1989

## Scanning Tunneling Microscopy of Nucleic Acids

GIL LEE, PATRICIA G. ARSCOTT, VICTOR A. BLOOMFIELD, D. FENNEL EVANS

The scanning tunneling microscope (STM) has been used to measure properties of poly(rA)·poly(rU) and DNA, such as helical pitch, half-period oscillations that were interpreted as the alternation between the major and minor grooves, and interhelical spacing. Average pitches were measured by two-dimensional Fourier transforms and by topographic profiles along the fiber axes. Values were typically 7 percent less than standard dimensions of A-form RNA and B-form DNA fibers. This result is compatible with the mild dehydration that occurred under air-drying conditions. More extensive dehydration typically led to 19 percent shrinkage. Analysis of specific regions allowed local variations in helical pitch as small as 1 angstrom to be detected, thus demonstrating that the STM can visualize functionally significant modulations of nucleic acid structure.

THE STM HAS ENABLED REMARKABLE visualization of surface topography with a vertical resolution of 0.2 Å and horizontal resolution of 2 to 3 Å (1). The possibility of visualizing nucleic acids at this high resolution has major significance, since the binding of proteins and other aspects of gene regulation depend on structural variations at the level of 1 Å (2). Conventional electron microscopy allows the local structure of individual molecules to be discerned, unlike fiber diffraction or solution techniques that average over entire molecules and populations of molecules. The STM offers an additional advantage in that contrast is achieved by detection of

sample height and work function variations, rather than by chemical treatments such as shadowing or staining. We report the use of the STM to measure the helical periodicities of air-dried double-stranded RNA and DNA molecules and in some cases to observe the alternation of major and minor grooves. Images of vacuum- and air-dried DNA were reported as early as 1984 by Binnig and Röhrer (3) and recently by Beebe *et al.* (4). However, these images were either obtained at low resolution or were so distorted that no reliable information could be obtained about helix dimensions. We show that nucleic acid dimensions and structural features can be quantitatively assessed and statistically analyzed by the STM, with small and reproducible corrections for hydration.

Calf thymus DNA (Sigma Chemical) and synthetic RNA, poly(rA)·poly(rU) (P-L Biochemicals, Milwaukee, Wisconsin) were purified and dissolved in a buffer of 1 mM

sodium cacodylate, 10 mM NaCl, pH 7.4, at a concentration of about 7  $\mu$ M nucleotide phosphate. To promote lateral association by charge neutralization, the DNA was mixed for 2 hours with 200  $\mu$ M spermidine HCl or 100  $\mu$ M hexaamine cobalt (III); stable RNA fiber bundles were obtained without these trivalent cations. We found that bundles, rather than individual molecules, gave the most regular and reproducible images, perhaps because of mutual stabilization of neighboring molecules under dehydrating conditions. One-drop samples were deposited on freshly cleaved, highly oriented pyrolytic graphite (HOPG, Union Carbide grade ZYA), and were air-dried at room temperature.

A Nanoscope II (Digital Instruments, Inc., Santa Barbara, California) equipped with a 9- $\mu$ m scan head made it possible to efficiently locate regions suitable for analysis but restricted the maximum magnification to areas 500 Å on a side (5). For most of the analysis, the digitized images were filtered to remove spike noise, narrow streaks, and the effects of sample tilt. Filtered and unfiltered images of poly(rA)·poly(rU) are shown in Fig. 1. Seven individual duplexes are readily discerned, and a repeat pattern is evident. A typical center-to-center distance between adjacent duplexes is  $24.8 \pm 0.8$  Å (R-5 in Table 1), which is only slightly greater than the 21.3 Å diameter of RNA (2). The vertical profile of the cross section is consistent with the bundle being composed of a single layer of RNA helices (Fig. 1A).

The filtered vertical displacement profile (Fig. 1E) along a helical molecule oscillates uniformly with a period corresponding to the pitch of A-RNA. The unfiltered profile (Fig. 1F) shows the same pattern but also

G. Lee and D. F. Evans, Department of Chemical Engineering and Materials Science and Interfacial Sciences Center, University of Minnesota, 100 Union Street, S.E., Minneapolis, MN 55455.

P. G. Arscott and V. A. Bloomfield, Department of Biochemistry, University of Minnesota, 1479 Gortner Avenue, St. Paul, MN 55108.

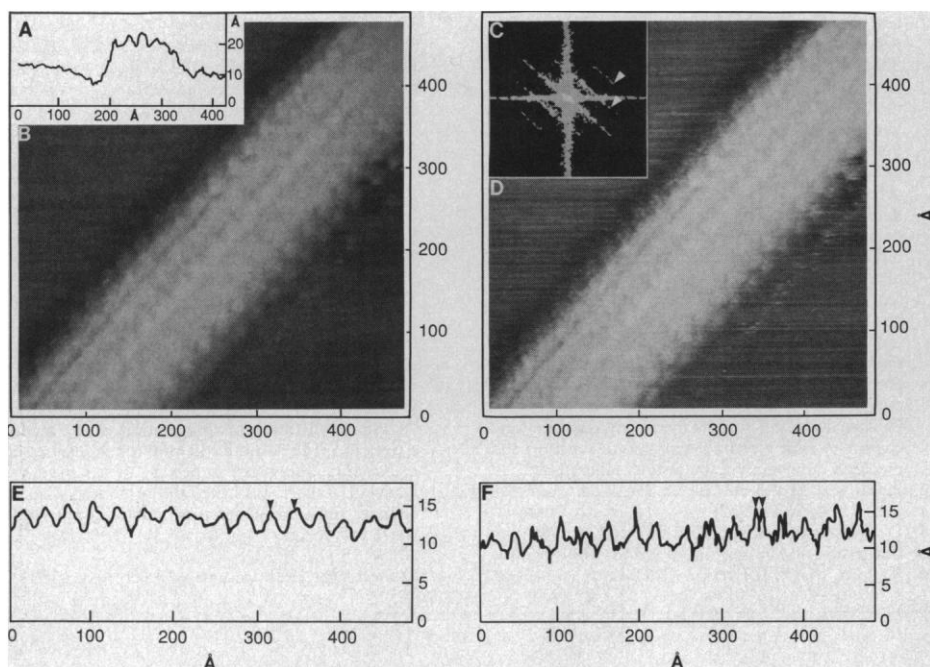


**Fig. 1.** STM image of a poly(rA)-poly(rU) bundle (R-5 in Table 1) containing seven duplexes with an average interhelical spacing of 24.8 Å. **(A)** Vertical profile perpendicular to fiber axis. **(B)** Filtered topographic image. **(C)** Two-dimensional Fourier transform, showing the first and second peaks at approximately 50° to the *x*-axis. **(D)** Unfiltered topographic image. **(E)** Vertical displacement profile along the second duplex from the right-hand side of the filtered image. The distance between the arrowheads is 29.5 Å. **(F)** Same as (E) but with the unfiltered image. The distance between the arrowheads is 7.0 Å.

**Table 1.** Analysis of STM images of RNA and DNA fiber bundles to obtain helix dimensions. The helix pitch was determined by the slope method. The filtered vertical displacement profile of each molecule in the bundle was measured over the portion of its image that allowed clear recording of regularly alternating peaks and troughs. The measurement was repeated three times to average over variations in placement of the cursor. Pitch was determined as the slope of the linear regression line of displacement along the fiber versus the number of peaks. The tabulated pitch is the average over all fibers in the bundle, weighted by the number of peak-to-peak distances measured ( $n_1$ ). The periodicities that correspond to maximum intensities of the two-dimensional Fourier transform peaks are those of the helix pitch (Per 1) and the major-minor groove alternation period (Per 2). The spacing is the distance between midlines of adjacent helices;  $n_2$  is the number of measurements. All of the RNA samples had 1 to 2 hours of drying, except R-7, which had 10 hours of drying. The DNA samples were prepared as follows: D-1 and D-2, no cations; D-3 through D-6, spermidine; and D-7, hexaammine cobalt (III), 10 hours drying.

| Sample | Bias (mV) | Pitch ( $n_1$ ) (Å) | Per 1 (Å) | Per 2 (Å) | Spacing $\pm$ SD ( $n_2$ ) (Å) |
|--------|-----------|---------------------|-----------|-----------|--------------------------------|
| R-1    | 31.4      | 28.7 (59)           | 28.6      | 14.3      | 24.7 $\pm$ 7.5 (5)             |
| R-2    | 43.6      | 29.7 (61)           | 29.7      | 14.1      | 20.9 $\pm$ 3.2 (18)            |
| R-3    | 43.6      | 29.1 (60)           | 29.2      | 14.8      | 29.3 $\pm$ 1.8 (17)            |
| R-4    | 27.8      | 28.1 (17)           | 28.1      | 13.7      | 21.9 $\pm$ 5.6 (5)             |
| R-5    | -34.8     | 30.0 (16)           | 29.5      | 14.4      | 24.8 $\pm$ 2.8 (8)             |
| R-6    | -60.1     | 26.9 (83)           | 26.5      | 14.4      | 21.4 $\pm$ 2.9 (4)             |
| R-7    | -46.7     | 23.3 (69)           |           |           |                                |
| D-1    | 81.2      | 29.2 (7)            |           |           |                                |
| D-2    | 52.5      | 30.1 (38)           |           |           |                                |
| D-3    | -73.2     | 31.4 (54)           | 30.7      | 15.8      | 30.7 $\pm$ 4.8 (58)            |
| D-4    | -73.2     | 30.4 (8)            | 30.4      | 14.8      | 32.0 $\pm$ 5.5 (16)            |
| D-5    | -73.2     | 32.4 (16)           | 33.3      | 15.9      | 29.3 $\pm$ 6.8 (20)            |
| D-6    | -85.1     | 31.5 (20)           |           |           |                                |
| D-7    | -69.6     | 22.8 (62)           |           |           | 19.9 $\pm$ 2.9 (18)            |

contains additional detail. Of particular interest are the two peaks, indicated by the arrows, that are separated by 7 Å, a value comparable to the width of the minor

groove (2). This spacing was observed in several other neighboring peaks of Fig. 1F, as well as in other samples that we analyzed.

Seven samples were analyzed with two

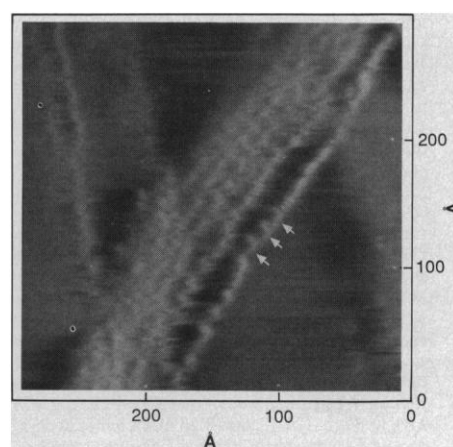


**Fig. 2.** STM image of a calf thymus DNA aggregate (D-1 in Table 1) without the presence of trivalent cation, which shows a single duplex separated from the main bundle. The structures oblique to the fiber bundle are steps on the cleaved graphite substrate. The three arrows point out features spaced at 34 Å. The average spacing in the bundle is 29.2 Å.

procedures to obtain information typical of the population of molecules (Table 1). A two-dimensional Fourier transform of the image (Fig. 1C) exhibited two peaks, one corresponding to the period of the helix and the other to the alternating major and minor grooves. The second method, or slope method, involves plotting the distance along the fiber axis as a function of the number of peaks traversed in the vertical displacement profile; the slope yields the helix periodicity and in most cases the half-period. The two procedures give values of the period that agree to within 0.1 Å. In samples R-1 through R-6, the period is  $28.7 \pm 1.1$  Å and the major-minor groove spacing is  $14.3 \pm 0.4$  Å.

The pitch of fully hydrated A-RNA determined by fiber diffraction is 30.9 Å (6), which is 7% greater than our STM value. Our samples were typically scanned in air for 1 to 2 hours, and are therefore expected to show mild dehydration, which is generally accompanied by shrinkage (7). In order to estimate the effects of dehydration, sample R-7 was dried for 10 hours. Its pitch is 19% less than the crystallographic value.

In Fig. 2 an aggregate of DNA is shown that was prepared without trivalent cations and that passed over a series of graphite ledges; a single helix is visible at the right of the aggregate. This structure is not as organized as RNA. The interhelical distance is variable and generally greater than the DNA diameter. Examination of this aggregate for several thousand angstroms on either side of the ledges revealed crossover of the strands, obscuring the pitch of the helices. Two analyses of the vertical displacement profiles of short segments gave periodicities of 29.2

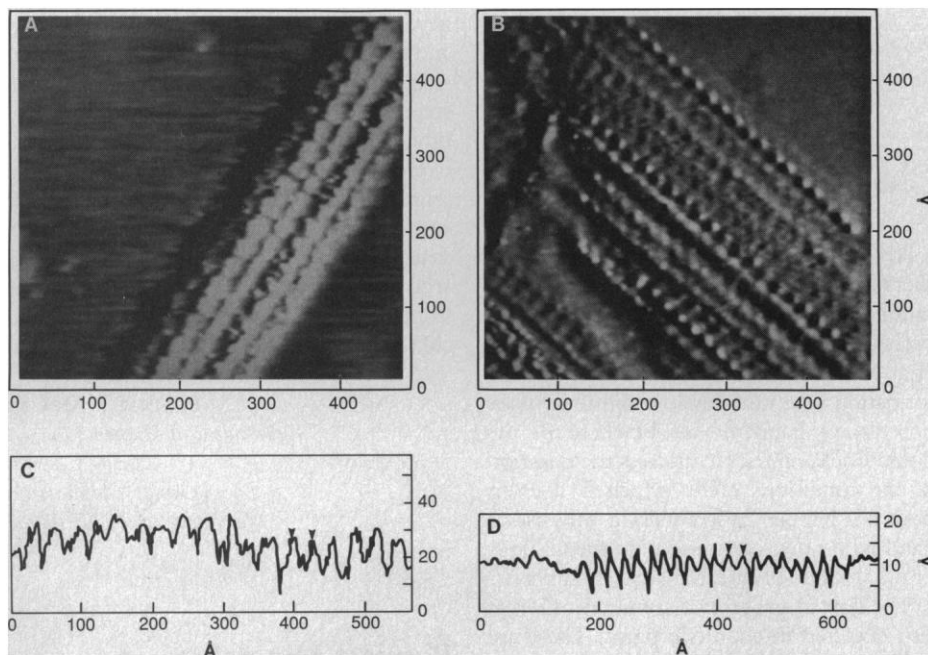


**Fig. 3.** STM images of calf thymus DNA, with lateral association induced by (A) spermidine (D-3 in Table 1) and (B) hexaammine cobalt (III) (D-7 in Table 1). The vertical displacement profiles give helical periods of (C) 31.8 Å and (D) 22.8 Å.

and 30.1 Å (Table 1, D-1 and D-2).

Suitable fiber bundles of DNA were obtained by treatment with spermidine (Fig. 3A) and hexaammine cobalt (III) (Fig. 3B). Analysis of samples D-3 to D-6 by Fourier transform and slope methods gave periodicities of  $31.5 \pm 1.3$  Å, a value 7% less than the 34 Å value expected for B-DNA. The hexaammine cobalt (III)-treated sample, D-7, has a periodicity of 22.8 Å, which is 19% less than the 28.2 Å expected for the A-DNA (2, 8). This large shrinkage is attributed to an extended drying time of ~10 hours. The effects of hydration have also been noted by Lindsay and co-workers (9), who obtained images of DNA samples submerged in water, and observed a double-helical pitch of 36 Å.

The features in the cross-sectional scan in

Fig. 1A—a depression on the left-hand side of the bundle and a suppressed height of the first helix on the right-hand side—are characteristic of STM imaging, and arise from the finite response time of the instrumental control loop as the probe is rastered from right to left across the bundle. In addition, vertical displacement is a complex function of probe-surface distance, work function, bias, scan rate, and other instrumental settings. There may also be an elastic interaction between sample and tip (9). Consequently, with inhomogeneous surfaces like RNA adsorbed on graphite, measured vertical displacements cannot be expected to correlate reliably with physical distances.

Several aspects of the STM imaging of nucleic acids deserve further comment. The Fourier transform method gives a rapid

average over the scanned field. Although the slope method is more tedious, it permits local changes in pitch to be determined. For example, the arrows in Fig. 2 point to features spaced at precisely the B-DNA repeat of 34 Å; other regions in this image and others show different periodicities. Thus variations in helical structure that accompany local base sequence, transitions between helical forms (for example, B-Z), or perturbations attendant upon protein binding can potentially be visualized.

#### REFERENCES AND NOTES

1. G. Binnig, H. Röhrer, C. Gerber, E. Weibel, *Phys. Rev. Lett.* **50**, 120 (1983); J. A. Golovchenko, *Science* **232**, 48 (1986); P. K. Hansma, V. B. Elings, O. Marti, C. E. Bracker, *ibid.* **242**, 209 (1988).
2. W. Saenger, *Principles of Nucleic Acid Structure* (Springer-Verlag, New York, 1984).
3. G. Binnig and H. Röhrer, in *Trends in Physics*, J. Janta and J. Pantoflíček, Eds. (European Physical Society, The Hague, 1984), p. 38; A. M. Baro *et al.*, *Nature* **315**, 253 (1985); G. Travaglini, H. Röhrer, M. Amrein, H. Gross, *Surf. Sci.* **181**, 380 (1987); M. Amrein, A. Stasiak, H. Gross, E. Stoll, G. Travaglini, *Science* **240**, 514 (1988).
4. T. P. Beebe, Jr., *et al.*, *Science* **243**, 370 (1989).
5. Probes were mechanically prepared from 90% Pt-10% Ir wire and were deemed acceptable only if they produced atomic resolution images of HOPG. In most cases, the instrument was operated in a constant current mode with set points ranging from 1.1 to 2.1 nA and bias voltages from -85 to 81 mV; the measured helix parameters were unaffected by bias.
6. V. Sasisekharan and P. B. Sigler, *J. Mol. Biol.* **12**, 296 (1965); S. Arnott, D. W. L. Hukins, S. D. Dover, *Biochem. Biophys. Res. Commun.* **48**, 1392 (1972).
7. D. Lang, H. T. Steely, Jr., C.-Y. Kao, N. Ktistakis, *Biochim. Biophys. Acta* **910**, 271 (1987).
8. S. Arnott, in *Proceedings of the First Cleveland Symposium on Macromolecules* A. G. Walton, Ed. (Elsevier, Amsterdam, 1977), pp. 87-104; M. T. Record, Jr., *et al.*, *Annu. Rev. Biochem.* **50**, 997 (1981).
9. S. M. Lindsay and B. Barris, *J. Vac. Sci. Technol.* **A6**, 544 (1988); B. Barris, U. Knipping, S. M. Lindsay, L. Nagahara, T. Thundat, *Biopolymers* **27**, 1691 (1988); S. M. Lindsay, T. Thundat, L. Nagahara, *J. Microsc.* **152**, 213 (1988); ———, in *Biological and Artificial Intelligence Systems*, E. Clementi and S. Chin, Eds. (ESCOM, Leiden, 1988), pp. 124-141.
10. Supported by NIH (GM 28093) and NSF (DMB 88-16433) grants to V.A.B. and NIH grant GM 34341 to D.F.E. and by the Center for Interfacial Engineering, an NSF Engineering Research Center.

18 January 1989; accepted 16 March 1989